Globule to Helix Transition in Sodiated Polyalanines

ARTICLE *in* JOURNAL OF PHYSICAL CHEMISTRY LETTERS · OCTOBER 2012

Impact Factor: 7.46 · DOI: 10.1021/jz301326w

6 AUTHORS, INCLUDING:

Jonathan K Martens
Radboud University Nijmegen
15 PUBLICATIONS **75** CITATIONS
SEE PROFILE

Terrance Mcmahon
University of Waterloo
206 PUBLICATIONS **5,443** CITATIONS
SEE PROFILE

Carine Clavaguéra
MINES ParisTech
57 PUBLICATIONS **725** CITATIONS
SEE PROFILE

Gilles Ohanessian
French National Centre for Scientific Research
115 PUBLICATIONS **3,709** CITATIONS
SEE PROFILE

THE JOURNAL OF PHYSICAL CHEMISTRY Letters

Letter

pubs.acs.org/JPCL

Globule to Helix Transition in Sodiated Polyalanines

Jonathan K. Martens,*[,†,‡] Isabelle Compagnon,[§] Edith Nicol,[†] Terry B. McMahon,[‡] Carine Clavaguéra,*[,†] and Gilles Ohanessian*[,†]

[†]Laboratoire des Mécanismes Réactionnels, Ecole Polytechnique, CNRS, 91128 Palaiseau Cedex, France

[‡]Department of Chemistry, University of Waterloo, Waterloo, Ontario, Canada, N2L 3G1

[§]Université de Lyon, F-69622, Lyon, France; Université Lyon 1, Villeurbanne, France; CNRS, UMR 5579, LASIM, Villeurbanne, France

Supporting Information

ABSTRACT: The structures of sodiated polyalanine peptides containing 8−12 residues are investigated using infrared multiple photon dissociation (IRMPD) spectroscopy and classical and quantum modeling. Calculations indicate that the α-helical structure is the most stable conformation for the peptides whatever their size. The IRMPD spectra provide evidence for the coexistence of helical and globular shapes for Ala_8Na^+, and possibly for Ala_9Na^+. The turning point from globule to helix is thus found at $Ala_{8-9}Na^+$. The N−H and O−H stretching region allows identifying a new spectroscopic pattern typical for α-helical structures of polyalanines.

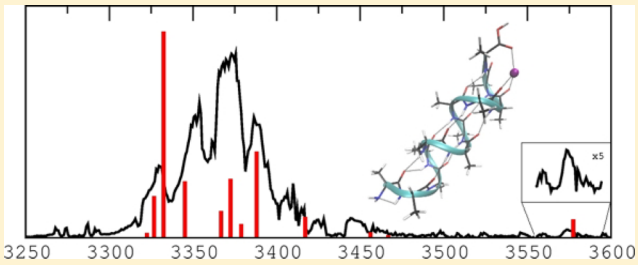

SECTION: Biophysical Chemistry and Biomolecules

Over 30% of amino acids in proteins exist in α-helical structures.[1] Their spectroscopic characterization in solution is well-established, in particular from the resulting vibrational bands in IR spectra.[2] Obtaining pure signatures of helices is made difficult by the instability of helical segments, when isolated in the form of short synthetic peptides.[3] When trying to further isolate the "intrinsic" spectroscopic signatures of helical segments from the influence of solvents, a gas phase approach is very appealing. Among well-known structural diagnostics in condensed phase (such as X-ray diffraction, NMR, and vibrational spectroscopy), IR absorption spectroscopy has been successfully transferred to the gas phase, in particular through the coupling of mass spectrometry with infrared multiple photon dissociation (IRMPD).[4] Yet, little is known to date about the infrared signatures of large gaseous peptides or small proteins with potential helical content.[5] Protonated polyalanines are a notable exception, for which a combination of measurements and calculations[6−8] yields convergent conclusions about structures being helical. Below we describe the results of a combination of IRMPD experiments and high-level quantum chemical calculations showing that signatures arising from α-helices can be obtained and identified at room temperature, and revealing the turning point from globules to helices with growing peptide size.

In metalloproteins, metal ions are often bound to α-helical segments. The ability of metal ions to stabilize helices in isolated peptides has been demonstrated by ion mobility spectrometry (IMS),[9,10] delineating the strong structural effects of electrical charges interacting with the helix macrodipole. In addition, IMS has been very successful in distinguishing globules or coils from helices.[10] Such studies, however, only provide a single experimental parameter, the drift time of a given structural type, and therefore lack specific, local information on how the molecule organizes in space. We show herein that IRMPD spectroscopy, when supported by accurate calculations, can provide such insight. We investigated sodiated polyalanines (containing 8−12 residues) known for their high helix propensity, and which can be compared to available IMS data,[9] indicating that helical structures may be favorable for sodiated polyalanines containing ca. 10 residues or more.

Attachment of a cation such as Na^+ to the C terminus of a helical segment is expected to lead to a large charge-dipole stabilizing interaction, despite a low three-coordination of the metal ion.[9] Other low energy structures can be formed with a peptide wrapped around the metal, optimizing ion "solvation" at the expense of breaking a large portion of the hydrogen bond network as compared to a helix. In order to reliably compare these two major structural types, extensive exploration of the potential energy surface must be carried out for each peptide size. To this end, replica exchange molecular dynamics (REMD) simulations were performed, followed by density functional theory (DFT) and ab initio refinement of the structures. The free energy and enthalpy of the most stable structure relative to the second lowest energy conformation are presented in Table 1 for each size. Our calculations indicate

Received: September 1, 2012
Accepted: October 26, 2012
Published: October 26, 2012

Table 1. Free Energies (kJ mol^{-1}, 298 K) of α-Helices Relative to the Second Lowest Energy Conformations[a]

	Ala_8Na^+	Ala_9Na^+	$Ala_{10}Na^+$	$Ala_{11}Na^+$	$Ala_{12}Na^+$
M06	−32.5	−41.5	−44.2	−21.9	−19.4
	(−20.4)	(−34.2)	(−38.0)	(−27.9)	(−16.9)
MP2(M06)	−25.4	−37.7	−38.6	−19.0	−10.1
	(−13.3)	(−30.5)	(−32.4)	(−25.1)	(−15.4)
CC2(M06)	−19.0	−32.9			
	(−6.8)	(−25.7)			
CC2(MP2)	−11.9				
	(−2.6)				

[a]Relative enthalpies are given in parentheses. M06 (M06/6-311+g-(d,p)//M06/6-31g(d,p)), MP2(M06) (RI-MP2/def2-TZVPP//M06/6-31g(d,p)), CC2(M06) (RI-CC2/def2-TZVPP//M06/6-31g(d,p)), CC2(MP2) (RI-CC2/def2-TZVPP//MP2/SVP).

that the most stable structure is fully α-helical for all sizes, and that the second conformation is globular for $Ala_{8-10}Na^+$ (i.e., with no periodic segment), whereas it is partially helical for $Ala_{11-12}Na^+$. No fully globular structure was identified at relatively low energy for $Ala_{11-12}Na^+$. For Ala_8Na^+, the α-helical and the lowest energy globular conformations are calculated to be very close in enthalpy at the highest level of theory, i.e., CC2(MP2), with an augmentation of the energy difference for $Ala_{9-10}Na^+$ as the size increases. The α-helical and globular structures of Ala_8Na^+ are shown in Figure 1 (for other sizes, see Figures S1−S4 in the Supporting Information). For purposes of description, we use sequence numbering from the N to the C terminus with superscripts, that is, NH^i and CO^i stand for the peptidic N−H and C═O bonds of the ith residue, respectively. It is found that the α-helical structures for all sizes share the following three features: (i) At the C-terminus, the sodium cation is coordinated with the C═O of the C-terminus in addition to C═O groups two and three residues earlier. The C═O group of the residue immediately preceding the C-terminal residue remains free. (ii) At the N-terminus, the NH_2 group interacts weakly with the NH^2. Additionally, the CO^1 forms hydrogen bonds with the NH^4 and NH^5, while the NH^3 is left free. (iii) All other residues are involved in typical α-helical hydrogen bonds of the $CO^n\cdots NH^{n+4}$ type.

Figure 2 shows the vibrational spectra of $Ala_{8-12}Na^+$ in the 3250−3600 cm^{-1} region, corresponding to N−H and O−H stretching modes. Ala_8Na^+ is clearly seen to be a mixture of isomers, where modes to the red of 3350 cm^{-1} (NH^5 at 3265 cm^{-1} and NH^4 at 3315 cm^{-1}), resulting from two short N−H···O═C hydrogen bonds, are contributed from the globular structure. The partly resolved bands match well to the calculated modes of the helical conformation in the 3340−3380 cm^{-1} segment, while a combination of bands predicted for the globule and the helix is required to account for the active blue part from 3380 to 3470 cm^{-1}. As for other sizes, NH^3 is free in the helix and found around 3460−3480 cm^{-1}. Finally, the free O−H mode at 3575 cm^{-1} is contributed by the helical structure and is distinct from the bound CO-H of the lowest energy globular structure (see Figure 1), predicted at 3329 cm^{-1}. For Ala_9Na^+, the calculated spectrum of the helix matches the experimental result well, except in the 3400−3450 cm^{-1} region, where the helical structure does not appear to fully suffice to reproduce the experimental spectrum. A mixture of both isomers cannot be excluded. In this case, the lowest energy globular structure also has a free O−H at 3575 cm^{-1}, making distinction on this basis impossible. For $Ala_{10}Na^+$, the calculated globular structure is clearly inconsistent with the experimental spectrum where the N−H stretching modes start at 3375 cm^{-1}, while the experimental pattern begins at approximately 3325 cm^{-1}. By contrast, the match is satisfactory for the α-helix. Thus a globular component can only be minor if any. For $Ala_{11}Na^+$, the spectrum computed for the helix matches well with experiment. In this case, the second structure is no longer globular, but it is partly helical instead. Its spectrum is thus more similar to that of the full helix than for smaller sizes; however, no band is calculated for this second structure in the 3330−3360 cm^{-1} range, making it a minor component at best. The calculated spectra shown for $Ala_{12}Na^+$ are both for entirely helical peptides, where only a small deviation (a break of the last hydrogen bond of the helix, where NH^{12} interacts with CO^{10} instead of CO^8) distinguishes them. Both computed spectra are consistent with experiments, which may indicate structural dynamics within globally stable helical patterns. The

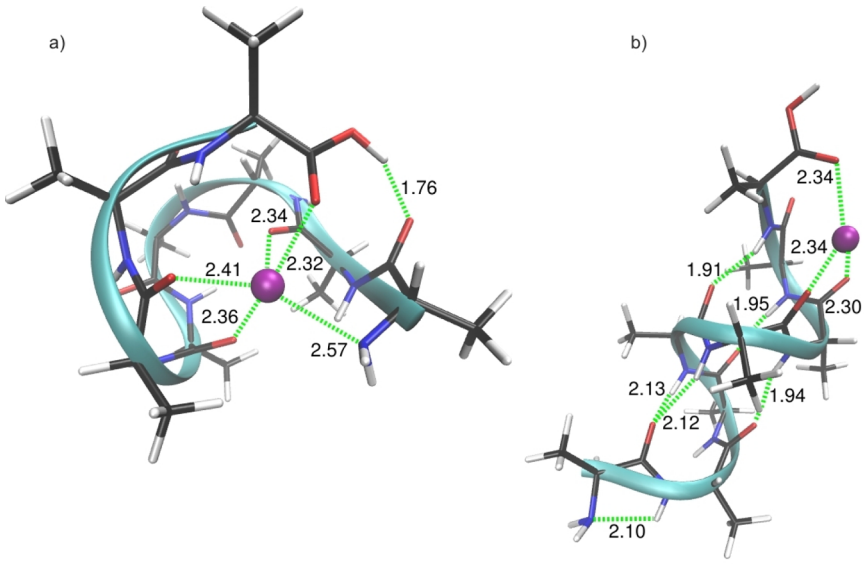

Figure 1. Ala_8Na^+: (a) lowest energy globular structure; (b) α-helical structure (lowest energy). M06/6-311+g(d,p)//M06/6-31g(d,p).

dx.doi.org/10.1021/jz301326w | J. Phys. Chem. Lett. 2012, 3, 3320−3324

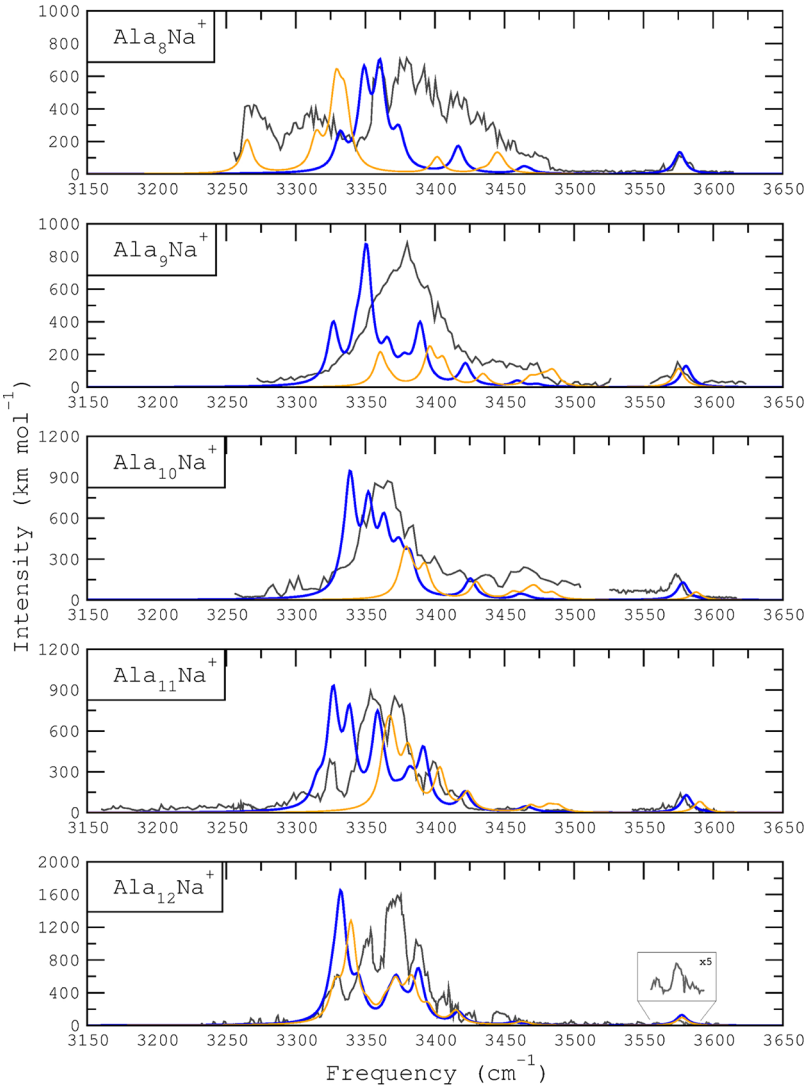

Figure 2. $Ala_{8-12}Na^+$ IRMPD OPO/OPA (3150−3650 cm^{-1}) spectra (solid line). M06/6-31g(d,p) calculated modes. Calculated spectra for the most stable structures (α-helix) are in blue, and those for the second lowest energy structures are in orange.

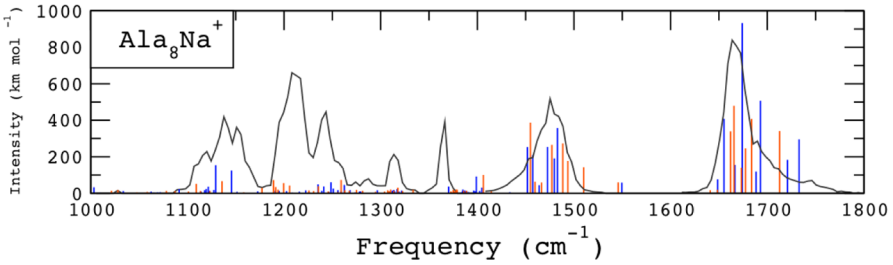

Figure 3. Ala_8Na^+ IRMPD spectrum (solid line). The calculated bar spectrum for α-helix is in blue, and that for lowest energy globular structure is in orange.

free O−H mode is calculated to be at 3575 cm^{-1} for both structures.

Interestingly, bound N−H frequencies are observed to be highly dependent on the hydrogen bonding distance, thus offering a refined structural diagnostic. For a given peptide, the shorter the N−H···O═C hydrogen bond, the smaller the N−H stretching frequency. Additionally, for α-helical conformations, calculated N−H···O═C hydrogen bond lengths decrease from the N-terminus (2.15 Å) to the C-terminus (1.89 Å), resulting in a consistent group of N−H stretching bands in the 3320−3420 cm^{-1} range. This pattern produces an α-helical signature, remaining very similar for peptides of different sizes, as clearly appearing in Figure 2. Furthermore, this pattern is quite sensitive to disruptions in the α-helical structure (especially at the C-terminus), as is well illustrated for the two calculated $Ala_{11}Na^+$ spectra. In the second lowest energy conformation, disruption of the helical structure at the C-terminus (favoring a larger extent of coordination of the sodium cation) prevents the short (1.89−1.94 Å) $NH^{11}\cdots OC^7$, $NH^{10}\cdots OC^6$, and $NH^9\cdots OC^5$ hydrogen bonds, that are present

dx.doi.org/10.1021/jz301326w | J. Phys. Chem. Lett. 2012, 3, 3320−3324

in the fully helical structure. This results in a blue shift of the N−H stretching band. In general, bound N−H modes are found between 3265 and 3445 cm^{-1}, and free N−H modes are between 3450 and 3490 cm^{-1}. The blue tail of the N−H massif in the 3430−3470 cm^{-1} range arises from the free peptidic N−H and the asymmetric NH_2 stretches. They are, however, too weak to be structurally diagnostic.

The spectrum in the fingerprint region for Ala_8Na^+ is shown in Figure 3. The band at 1640−1765 cm^{-1} (including the amide I massif and the carboxyl C═O stretching band) is calculated to extend farther to the blue for the helical structure than for the globular structure, due to the free carboxylic C═O as well as the free amide C═O of the second to last residue. This feature is characteristic of helices of all sizes (spectra not shown). It is clearly illustrated in the experimental spectrum of Ala_8Na^+, where the band extends to 1765 cm^{-1}, nearly 50 cm^{-1} farther than the last mode of the calculated spectrum of the globular structure. The amide II band (mainly N−H modes, 1450−1500 cm^{-1}) matches both calculated structures, thus being nondiagnostic. For Ala_8Na^+, the coexistence of a globular form accounts for the active region around 1200−1250 cm^{-1}, and possibly near 1310 cm^{-1}.

Our results in the fingerprint region, which is commonly used for structural characterization of proteins in solution, confirm that the amide I band allows distinguishing helices from globules, whereas the amide II is less diagnostic. In the N−H and O−H stretching region, which is obscured by water bands in aqueous solution, we identify more spectrally resolved features, offering a refined structural diagnostic. α-helical structures with a three-coordination of the metal cation at the C-terminus are computed to be the most stable forms for all sizes. Although stable globules coexist for Ala_8Na^+, the energy difference between these two forms increases with the size of the peptide, to the point where low-energy globules are no longer found in the conformational exploration (sizes 11−12). These results indicate that the size dependent transition from globular to α-helical structures in sodiated polyalanine is found at $Ala_{8-9}Na^+$, refining previous findings from Jarrold et al.,[10] and extending them by differentiating partly from fully helical structures in the N−H and O−H stretching region. It is, however, not possible to assign individual structures to the experimental spectra, probably due in part to the limited experimental resolution, and to dynamical behavior of hydrogen bond networks at room temperature. Comparison of these results to those obtained previously for Gly_n[11] is also informative. Indeed, Ala is known to have the highest helix propensity of all amino acid residues in solution, while Gly has the lowest. Although the small sodiated peptides (2−4 residues) have similar structures for Ala_n and Gly_n,[12,13] Ala_8Na^+ has the full helix and a globule as lowest-energy structures, while for Gly_8Na^+ the helix is much higher in energy. This parallels the trend in solution, indicating that the latter does not arise from solvation effects only. In addition, for these 8-mers, the lowest-energy globules are found to be different, suggesting that the smaller steric crowding in Gly_n versus Ala_n may have an enthalpic as well as entropic contribution to the trend in relative free energies.[14] This divergence highlights the subtlety of the balance between the various intrinsic and environmental effects leading to the stabilization of a particular secondary structure. These results show that, despite spectral congestion, combination of IRMPD spectroscopy and state-of-the-art calculations is a powerful tool to decipher the structure of medium-sized peptides.

EXPERIMENTAL AND COMPUTATIONAL SECTION

IRMPD spectra were obtained at the Centre Laser Infrarouge d'Orsay (CLIO).[15] A free electron laser (FEL) and an optical parametric oscillator/amplifier (OPO/OPA) were used for the fingerprint (1000−1800 cm^{-1}) and 3250−3600 cm^{-1} regions, respectively, both coupled to the 7T Fourier transform ion cyclotron resonance (FT-ICR) mass spectrometer described previously.[16−18] In both experiments, a continuous wave broadband CO_2 laser was used to enhance fragmentation ratios as has also been previously described.[19,20] Ions were generated by electrospray ionization from solutions prepared by dissolving the peptide sample (GeneCust-Luxembourg in unpurified but desalted form) in a small amount of trifluoroacetic acid, followed by dilution in trifluoroethanol. Obtaining satisfactory fragmentation yields turned out to be difficult in both spectral ranges. For the OPO/OPA experiments, essentially zero fragmentation was observed with either the OPO/OPA or CO_2 laser alone, while in combination, fragmentation yields, of approximately 0.1−0.3, were observed with 5−10 s irradiation times. The extent of fragmentation is expressed as the fragmentation efficiency, F_{eff}, defined as $F_{eff} = -\log[I_p/(I_p + \sum I_{frag})]$, in which I_p and I_{frag} are the parent and fragment ion intensities, respectively. For the FEL experiments, use of the CO_2 laser was beneficial and allowed the use of shorter irradiation times, although fragmentation was observed under FEL irradiation only, however, with harsh irradiation conditions.

REMD simulations incorporating the polarizable AMOEBA force field[21,22] were performed as detailed previously[11,23] to explore the potential energy surface of the peptides. A selection of ca. 30 AMOEBA-optimized structures was refined at several successive DFT and ab initio levels. The role of dispersion interactions in shaping peptide structures, and in particular in stabilizing helices, being crucial,[8] B3LYP-D and M06 functionals were used for all DFT calculations. Final M06/6-31g(d,p) geometries and frequencies and M06/6-311+g(d,p) final energetic results are presented for the most stable structures at each peptide size. Reference energies at the RI-MP2/def2-TZVPP and RI-CC2/def2-TZVPP energies on the M06 geometries were also computed. Furthermore, a selection was considered at the RI-MP2/def2-TZVPP//RI-MP2/def2-SVP level for benchmarking purposes. M06 vibrational analysis was previously found to be very consistent with experimental results on other peptides.[24,25] Harmonic vibrational modes were scaled by 0.940 and 0.955, in the 1000−1800 and 3000−3600 cm^{-1} ranges, respectively. Calculations were performed using TURBOMOLE 6.1[26] and Gaussian 09[27] packages. The calibration of methods presented in Table 1 highlights an overestimation by standard levels of the energy difference between fully helical and globular structures in the $Ala_{8-10}Na^+$ cases. The error is expected to decrease for $Ala_{11-12}Na^+$ because the two structures are much more similar to each other. Even if free energies are naturally preferred for comparison with experiments, the relative enthalpies are also provided due to uncertainties in the entropy calculation. Free energies and enthalpies yield similar trends in the comparisons of either peptide sizes or computational levels for a given size.

dx.doi.org/10.1021/jz301326w | J. Phys. Chem. Lett. 2012, 3, 3320−3324

■ ASSOCIATED CONTENT

Supporting Information

Figures including the two lowest energy structures for Ala_9Na^+ to $Ala_{12}Na^+$. This material is available free of charge via the Internet at http://pubs.acs.org.

■ AUTHOR INFORMATION

Corresponding Author

*E-mail: j2marten@uwaterloo.ca (J.K.M.); carine.clavaguera@polytechnique.edu (C.C.); gilles.ohanessian@polytechnique.fr (G.O.).

Notes

The authors declare no competing financial interest.

■ ACKNOWLEDGMENTS

Use of the FT-ICR mass spectrometer at Orsay was supported by the TGE "Spectrométrie de masse FT-ICR à très haut champ" funded by the CNRS Institute of Chemistry. We are grateful to the CLIO team for their excellent technical support during experiments. J.K.M. thanks the vice-presidency for external relations in École Polytechnique for support from the international internship program. This work was supported by the CNRS through the "Groupement de Recherche GDR 2758". This work was granted access to the HPC resources of [CCRT/CINES/IDRIS] under the allocation c2012085107 made by GENCI (Grand Equipement National de Calcul Intensif)

■ REFERENCES

(1) Barlow, D. J.; Thornton, J. M. Helix Geometry in Proteins. *J. Mol. Biol.* **1988**, *201*, 601−619.

(2) Siebert, F.; Hildebrandt, P. *Vibrational spectroscopy in Life Science*; Wiley-VCH: Weinheim, Germany, 2007.

(3) Scholtz, J. M.; Baldwin, R. L. The Mechanism of α-Helix Formation by Peptides. *Annu. Rev. Biophys. Biomol. Struct.* **1992**, *21*, 95−118.

(4) Polfer, N. C.; Oomens, J. Vibrational Spectroscopy of Bare and Solvated Ionic Complexes of Biological Relevance. *Mass Spectrom. Rev.* **2009**, *28*, 468−494.

(5) Oomens, J.; Polfer, N.; Moore, D. T.; van der Meer, L.; Marshall, A. G.; Eyler, J. R.; Meijer, G.; von Helden, G. Charge-State Resolved Mid-infrared Spectroscopy of a Gas-Phase Protein. *Phys. Chem. Chem. Phys.* **2005**, *7*, 1345−1348.

(6) Stearns, J. A.; Boyarkin, O. V.; Rizzo, T. R. Spectroscopic Signatures of Gas-Phase Helices: Ac-Phe-$(Ala)_5$-Lys-H^+ and Ac-Phe-$(Ala)_{10}$-Lys-H^+. *J. Am. Chem. Soc.* **2007**, *129*, 13820−13821.

(7) Rossi, M.; Blum, V.; Kupser, P.; von Helden, G.; Bierau, F.; Pagel, K.; Meijer, G.; Scheffler, M. Secondary Structure of Ac-Ala_n-LysH^+ Polyalanine Peptides (n = 5,10,15) in Vacuo: Helical or Not? *J. Phys. Chem. Lett.* **2010**, *1*, 3465−3470.

(8) Tkatchenko, A.; Rossi, M.; Blum, V.; Ireta, J.; Scheffler, M. Unraveling the Stability of Polypeptide Helices: Critical Role of van der Waals Interactions. *Phys. Rev. Lett.* **2011**, *106*, 118102.

(9) Kohtani, M.; Kinnear, B. S.; Jarrold, M. F. Metal-Ion Enhanced Helicity in the Gas Phase. *J. Am. Chem. Soc.* **2000**, *122*, 12377−12378.

(10) Jarrold, M. F. Helices and Sheets in Vacuo. *Phys. Chem. Chem. Phys.* **2007**, *9*, 1659−1671.

(11) Balaj, O.; Semrouni, D.; Steinmetz, V.; Nicol, E.; Clavaguéra, C.; Ohanessian, G. Structure of Sodiated Polyglycines. *Chem.—Eur. J.* **2012**, *18*, 4583−4592.

(12) Balaj, O. P.; Kapota, C.; Lemaire, J.; Ohanessian, G. Vibrational Signatures of Sodiated Oligopeptides (GG-Na^+, GGG-Na^+, AA-Na^+ and AAA-Na^+) in the Gas Phase. *Int. J. Mass Spectrom.* **2008**, *269*, 196−209.

(13) Wang, P.; Wesdemiotis, C.; Kapota, C.; Ohanessian, G. The Sodium Ion Affinities of Simple Di-, Tri-, and Tetrapeptides. *J. Am. Soc. Mass Spectrom.* **2007**, *18*, 541−552.

(14) Chakrabartty, A.; Baldwin, R. L. Stability of α-Helices. *Adv. Protein Chem.* **1995**, *46*, 141−176.

(15) Maître, P.; Caër, S. L.; Simon, A.; Jones, W.; Lemaire, J.; Mestdagh, H.; Heninger, M.; Mauclaire, G.; Boissel, P.; Prazeres, R.; et al. Ultrasensitive Spectroscopy of Ionic Reactive Intermediates in the Gas Phase Performed with the First Coupling of an IR FEL with an FTICR-MS. *Nucl. Instrum. Methods Phys. Res., Sect. A* **2003**, *507*, 541−546.

(16) MacAleese, L.; Maître, P. Infrared Spectroscopy of Organometallic Ions in the Gas Phase: From Model to Real World Complexes. *Mass Spectrom. Rev.* **2007**, *26*, 583−605.

(17) Bakker, J. M.; Besson, T.; Lemaire, J.; Scuderi, D.; Maître, P. Gas-Phase Structure of a π-Allyl-Palladium Complex: Efficient Infrared Spectroscopy in a 7 T Fourier Transform Mass Spectrometer. *J. Phys. Chem. A* **2007**, *111*, 13415−13424.

(18) Bakker, J. M.; Sinha, R. K.; Besson, T.; Brugnara, M.; Tosi, P.; Salpin, J.-Y.; Maître, P. Tautomerism of Uracil Probed via Infrared Spectroscopy of Singly Hydrated Protonated Uracil. *J. Phys. Chem. A* **2008**, *112*, 12393−12400.

(19) Sinha, R. K.; Nicol, E.; Steinmetz, V.; Maître, P. Gas Phase Structure of Micro-hydrated $[Mn(ClO_4)]^+$ and $[Mn_2(ClO_4)_3]^+$ Ions Probed by Infrared Spectroscopy. *J. Am. Soc. Mass Spectrom.* **2010**, *21*, 758−772.

(20) Scuderi, D.; Bakker, J.; Durand, S.; Maître, P.; Sharma, A.; Martens, J.; Nicol, E.; Clavaguéra, C.; Ohanessian, G. Structure of Singly Hydrated, Protonated Phospho-Tyrosine. *Int. J. Mass Spectrom.* **2011**, *308*, 338−347.

(21) Ren, P.; Ponder, J. W. Consistent Treatment of Inter- and Intramolecular Polarization in Molecular Mechanics Calculations. *J. Comput. Chem.* **2002**, *23*, 1497−1506.

(22) Ponder, J. W. TINKER - Software Tools for Molecular Design, 2010; http://dasher.wustl.edu/tinker.

(23) Semrouni, D.; Balaj, O.; Calvo, F.; Correia, C.; Clavaguéra, C.; Ohanessian, G. Structure of Sodiated Octa-glycine: IRMPD Spectroscopy and Molecular Modeling. *J. Am. Soc. Mass Spectrom.* **2010**, *21*, 728−738.

(24) Semrouni, D.; Clavaguéra, C.; Dognon, J.-P.; Ohanessian, G. Assessment of Density Functionals for Predicting the Infrared Spectrum of Sodiated Octa-glycine. *Int. J. Mass Spectrom.* **2010**, *297*, 152−161.

(25) Joshi, K.; Semrouni, D.; Ohanessian, G.; Clavaguéra, C. Structures and IR Spectra of the Gramicidin S Peptide: Pushing the Quest for Low-Energy Conformations. *J. Phys. Chem. B* **2012**, *116*, 483−490.

(26) Ahlrichs, R.; Bar, M.; Haser, M.; Horn, H.; Kolmel, C. Electronic-Structure Calculations on Workstation Computers - The Program System TURBOMOLE. *Chem. Phys. Lett.* **1989**, *162*, 165−169 for the current version, see http://www.turbomole.com.

(27) Frisch, M. J.; Trucks, G. W.; Schlegel, H. B.; Scuseria, G. E.; Robb, M. A.; Cheeseman, J. R.; Scalmani, G.; Barone, V.; Mennucci, B.; Petersson, G. A. et al. *Gaussian 09*, revision A.1; Gaussian Inc.: Wallingford, CT, 2009.